CrossMark

J. Fluid Mech. (2021), *vol*. 926, R2, doi:10.1017/jfm.2021.741

Added-mass force on elliptic airfoils

Eric J. Limacher†

Department of Mechanical and Aerospace Engineering, Princeton University, Princeton, NJ 08544, USA

(Received 6 May 2021; revised 11 July 2021; accepted 16 August 2021)

Herein, exact algebraic expressions for the non-circulatory (added-mass) forces on elliptic airfoils are derived for any two-dimensional motion – including simultaneous rectilinear acceleration and rotation – embedded in a steady free-stream flow. Despite the lengthy history of the added-mass concept and its widespread application to cylinders of various cross-sections, such closed-form expressions for elliptic cylinders, in terms of kinematic and geometric parameters alone, have remained absent from the literature until now. Inspection of the derived equations reveals that for pure pitching about a point on the chord-line, increasing thickness always decreases the added-mass force magnitude. For any given motion of the chord-line, the difference in force between thick and thin airfoils is proportional to the square of the thickness, although this difference may be positive or negative for the general three-degree-of-freedom case. In the special case of zero thickness and small pitch angles, Theodorsen's added-mass lift force on rigid thin airfoils is recovered; for large pitch angles, an exact generalization of Theodorsen's expression, applicable to the chord-normal direction, is given.

Key words: aerodynamics

1. Introduction

The decomposition of force into circulatory and non-circulatory components is widely used in aerodynamic modelling. This decomposition heralds back to the pioneers of thin-airfoil theory in the first half of the twentieth century, e.g. Theodorsen (1935) and von Kármán & Sears (1938). The circulatory component is related to the evolution of the surrounding vorticity field, and the non-circulatory component is derived from the hypothetical acyclic (i.e. single-valued) potential flow around the body. The non-circulatory force is often referred to as the added-mass force because, in the special case of rectilinear translation, it is proportional to instantaneous acceleration, manifesting 'as if' additional mass were accelerated with the body (Brennen 1982). For more general motions, this analogy breaks down; in coupled translation and rotation, for example, forces normal to the translational direction arise. Somewhat confusingly, the totality of

† Email address for correspondence: limacher@princeton.edu

© The Author(s), 2021. Published by Cambridge University Press

https://doi.org/10.1017/jfm.2021.741 Published online by Cambridge University Press

non-circulatory force contributions is referred to in the literature as ‘added-mass forces’, and herein this nomenclature is perpetuated, with some reservation, to ensure that the work reaches the intended audience.

The confusion surrounding added mass goes deeper still, owing to the existence of two competing definitions of the added-mass force. Limacher (2019) distinguished between the *classical* added-mass force, as described in the previous paragraph, and the *empirical* added-mass force. Empirical added-mass coefficients are derived from experiments in which a body is oscillated at various frequencies, and the force response is fitted to a second-order ordinary differential equation, treating the combined fluid–body system as a mass-spring-damper analogue, e.g. Fackrell (2011). The coefficient on the second-order term is then designated the added mass (or added-mass coefficient).

The overarching goal to which this work contributes is the rigorous extension of unsteady airfoil theory to account for large-amplitude oscillations and airfoils of any cross-section. Accordingly, the classical added-mass force is treated herein, which can be superimposed onto the circulatory force to give the total force exactly. This superposition was originally derived for potential flows with embedded vortex singularities, but was recently shown to hold for viscous, incompressible flows as well (Limacher, Morton & Wood 2018).

The primary contribution of the present work is the derivation of an exact algebraic expression for the added-mass force on elliptic airfoils undergoing any two-dimensional motion, immersed in a steady free-stream flow. From there, in the special case of zero airfoil thickness, an exact generalization of Theodorsen’s added-mass expression is derived, valid for any pitch angle. Then, for a few canonical harmonic motions – pure pitching, pure plunging, and combined pitching and plunging – the effect of airfoil thickness on the added-mass force is discussed.

The present derivation approach starts with the known classical added-mass forces on an ellipse in rectilinear motion (Brennen 1982) and presents a framework to generalize to any motion whatsoever. This framework is applicable to other rotationally symmetric two-dimensional bodies for which the added-mass force is known in response to two orthogonal components of linear acceleration. It must be emphasized, however, that this method of generalization takes strictly non-circulatory forces as inputs. Empirical added-mass coefficients may implicitly contain both circulatory and non-circulatory contributions (Williamson & Govardhan 2004). Even added-mass forces derived from potential flow analysis may contain a circulatory component if they are derived with vortex singularities inside or along the airfoil surface. La Mantia & Dabnichki (2012), for example, derive forces on symmetric airfoils from numerically obtained potential flow solutions, but they introduce a circulatory component by enforcing the Kutta condition at the trailing edge. Of course, it is not immediately clear how to avoid this contamination, as solving for the acyclic potential flow around an airfoil with a sharp trailing edge would be numerically challenging. The consideration of elliptic airfoils in the present work avoids this complication while still offering preliminary insight into the effect of airfoil thickness.

Recently, Fernandez-Feria (2019) derived expressions for the total aerodynamic force and moment on elliptic bodies using the force decomposition method developed by Quartapelle & Napolitano (1983) and Chang (1992). Fernandez-Feria groups the resulting force terms into what he labels ‘vortical’ and ‘added-mass’ components. Although these groupings differ in form from the circulatory and non-circulatory forces derived using vortical impulse theory (Limacher *et al.* 2018), Fernandez-Feria’s work does treat the scalar potential field surrounding the body, and so falls squarely within the classical category of added-mass treatments. Even within that category, subtle definitional differences remain to be resolved, as will be briefly discussed herein. In any case, the

https://doi.org/10.1017/jfm.2021.741 Published online by Cambridge University Press

present work complements Fernandez-Feria's efforts by presenting an (arguably) more accessible derivation; by including the effect of a non-zero free-stream velocity; and by expressing the classical added-mass force entirely in terms of geometric and kinematic parameters.

2. Derivation

The general expression of the classical added-mass force, $\boldsymbol{F}$, for any two-dimensional body with a piecewise-continuous outer contour, S, undergoing arbitrary motion in an unbounded incompressible fluid is given as (Limacher *et al.* 2018)

$$\boldsymbol{F} = -\rho \frac{\mathrm{d}}{\mathrm{d}t}(\boldsymbol{P}_\phi + \boldsymbol{P}_b), \tag{2.1}$$

where ρ is the fluid density, $\mathrm{d}/\mathrm{d}t$ denotes differentiation with respect to time, and $\boldsymbol{P}_\phi$ and $\boldsymbol{P}_b$ are the potential impulse and the body-volume impulse, respectively. They are defined as

$$\boldsymbol{P}_\phi = -\oint_S \boldsymbol{n}\phi' \,\mathrm{d}S, \tag{2.2}$$

$$\boldsymbol{P}_b = -\boldsymbol{u}_c A, \tag{2.3}$$

where $\boldsymbol{n}$ is the outward-facing normal on S (pointing into the fluid), $\boldsymbol{u}_c$ is the instantaneous velocity of the body centroid and A is the cross-sectional area of the body.

The quantity ϕ' is the scalar potential describing the irrotational component of the velocity field according to $\boldsymbol{u}'_\phi = \nabla\phi'$, where $\boldsymbol{u}'_\phi$ is defined in a frame of reference relative to the body centroid (prime superscripts denote the body-fixed frame of reference, consistent with the notation of Limacher *et al.* (2018)). Although (2.2) only requires ϕ' to be known on S, it must be obtained as the solution to the Laplace equation on a two-dimensional domain. When solving for $\nabla^2\phi' = 0$ on the fluid domain outside the body, the solution is subject to the boundary condition $\nabla\phi' = \boldsymbol{U}_\infty - \boldsymbol{u}_c$ at infinity, where $\boldsymbol{U}_\infty$ is the steady free-stream velocity far from the body, and the impermeable boundary condition $\boldsymbol{n}\cdot\nabla\phi' = 0$ on S.

An equivalent added-mass formulation is given by Saffman (1992), although he treats the scalar potential describing the velocity in the absolute frame of reference. Of course, the choice of reference frame used in the derivation is immaterial to the final results, but a useful aspect of the approach of Limacher *et al.* (2018) is in the comparison it facilitates to the seminal work of Wu (1981). Wu's exact and general expression of aerodynamic force in terms of body motion, body geometry and vorticity-field evolution has instigated decades of intervening interest in what we now call *vortical impulse theory*, for which Wu, Ma & Zhou (2015) is recommended as an authoritative reference.

One further note on boundary conditions is warranted, highlighting definitional differences within the category of classical added-mass analyses. In Limacher *et al.* (2018), and above, the boundary condition for ϕ' on S does not include the surface-normal velocity component due to body rotation, in contrast to other treatments of the classical added-mass force and moment, e.g. La Mantia & Dabnichki (2012), Fernandez-Feria (2019). The reason for this difference in treatment is explained in the Appendix, where it is also shown to have no effect on the force expressions derived for elliptic airfoils (or for any other rotationally symmetric body).

Two coordinate systems will be employed in the present analysis: an inertial coordinate system (X, Y), with the X- and Y-directions aligned stream-wise and stream-normal,

https://doi.org/10.1017/jfm.2021.741 Published online by Cambridge University Press

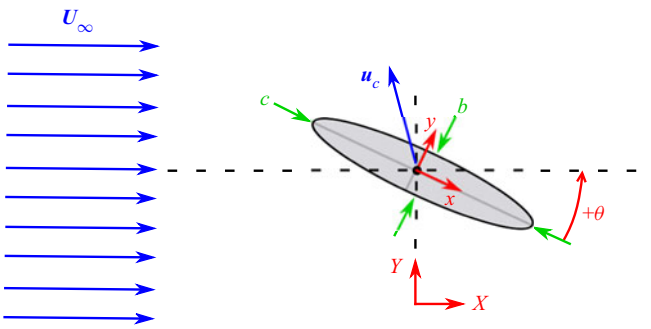

Figure 1. Inertial (X, Y) and body-fixed (x, y) coordinate systems used in the present analysis. Here, c is airfoil chord length (major axis length), b is airfoil thickness (minor axis length), θ is the pitch angle (positive in the sense shown) relative to the free stream, $\boldsymbol{U}_\infty$, and $\boldsymbol{u}_c$ is the velocity of the airfoil centroid (i.e. the mid-chord).

respectively; and a body-fixed coordinate system (x, y), with the x- and y-directions aligned with the major and minor axes of the ellipse, respectively (see figure 1). Throughout the paper, uppercase subscripts (X or Y) refer to vector components in the inertial frame, and lowercase subscripts (x or y) to the body-fixed frame. At any instant in time, the angle from the x-axis to the X-axis is θ (positive counterclockwise).

Now, it would be possible to solve for the potential impulse on the ellipse as a function of $\boldsymbol{u}_c$ and θ using standard potential flow techniques. One could, for example, take the known complex potential around a circle and relate it to the domain around an ellipse by means of a conformal map (Milne-Thomson 1968). Or, for any body of interest, the potential flow could be solved computationally, thereafter numerically approximating the integral in (2.2). Fortunately, such efforts can be avoided for the ellipse case, as the known added-mass forces for linear acceleration yield sufficient information when combined with (2.1)–(2.3). These known forces are as follows (Brennen 1982):

$$F_x = -\frac{\pi\rho b^2}{4}\frac{\mathrm{d}u_{cx}}{\mathrm{d}t}, \tag{2.4}$$

$$F_y = -\frac{\pi\rho c^2}{4}\frac{\mathrm{d}u_{cy}}{\mathrm{d}t}, \tag{2.5}$$

where c is the airfoil chord (ellipse major axis length), b is the airfoil thickness (ellipse minor axis length), and $\mathrm{d}u_{cx}/\mathrm{d}t$ and $\mathrm{d}u_{cy}/\mathrm{d}t$ are the chord-wise and chord-normal components of the mid-chord acceleration, respectively.

Before making use of these expressions, let us further clarify how the components of impulse are related to the components of force. The stream-normal and stream-wise forces are

$$\frac{1}{\rho}\begin{bmatrix}F_X\\F_Y\end{bmatrix} = -\frac{\mathrm{d}}{\mathrm{d}t}\begin{bmatrix}P_{\phi X}\\P_{\phi Y}\end{bmatrix} + \frac{\pi bc}{4}\frac{\mathrm{d}}{\mathrm{d}t}\begin{bmatrix}u_{cX}\\u_{cY}\end{bmatrix}, \tag{2.6}$$

where the area of an ellipse $A = \pi bc/4$ has been substituted. It will prove more convenient to treat the chord-wise and chord-normal forces, related to the stream-normal and stream-wise forces by a rotation matrix, $\boldsymbol{R}(\theta)$:

$$\boldsymbol{R}(\theta) = \begin{bmatrix}\cos\theta & -\sin\theta\\ \sin\theta & \cos\theta\end{bmatrix}. \tag{2.7}$$

https://doi.org/10.1017/jfm.2021.741 Published online by Cambridge University Press

This allows us to write

$$\frac{1}{\rho}\begin{bmatrix}F_x\\F_y\end{bmatrix} = \boldsymbol{R}(\theta)\frac{\mathrm{d}}{\mathrm{d}t}\left\{\boldsymbol{R}(-\theta)\left(-\begin{bmatrix}P_{\phi x}\\P_{\phi y}\end{bmatrix}+\frac{\pi bc}{4}\begin{bmatrix}u_{cx}\\u_{cy}\end{bmatrix}\right)\right\}. \tag{2.8}$$

If we apply the product rule and note that

$$\boldsymbol{R}(\theta)\frac{\mathrm{d}\boldsymbol{R}(-\theta)}{\mathrm{d}t} = \frac{\mathrm{d}\theta}{\mathrm{d}t}\begin{bmatrix}0 & 1\\-1 & 0\end{bmatrix}, \tag{2.9}$$

then (2.8) becomes

$$\frac{1}{\rho}\begin{bmatrix}F_x\\F_y\end{bmatrix} = -\frac{\mathrm{d}\theta}{\mathrm{d}t}\begin{bmatrix}P_{\phi y}\\-P_{\phi x}\end{bmatrix}-\frac{\mathrm{d}}{\mathrm{d}t}\begin{bmatrix}P_{\phi x}\\P_{\phi y}\end{bmatrix}+\frac{\pi bc}{4}\left\{\frac{\mathrm{d}\theta}{\mathrm{d}t}\begin{bmatrix}u_{cy}\\-u_{cx}\end{bmatrix}+\frac{\mathrm{d}}{\mathrm{d}t}\begin{bmatrix}u_{cx}\\u_{cy}\end{bmatrix}\right\}, \tag{2.10}$$

demonstrating how rotation causes the impulse components to contribute perpendicular force components.

For rectilinear motion in still fluid, $\mathrm{d}\theta/\mathrm{d}t = 0$, and we can solve for the potential impulse by substituting the force expressions in (2.4) and (2.5) into (2.10) and taking the antiderivative with respect to time, yielding

$$P_{\phi x} = \frac{\pi}{4}b(b+c)u_{cx}; \quad P_{\phi y} = \frac{\pi}{4}c(b+c)u_{cy}. \tag{2.11a,b}$$

To generalize these expressions in the presence of a free-stream flow, and to allow for a variable pitch angle relative to that flow, recall that the scalar potential in (2.2) is solved for the boundary condition $\nabla\phi' = \boldsymbol{U}_\infty - \boldsymbol{u}_c$ at infinity. Accordingly, we replace u_{cx} and u_{cy} with $u_{cx} - U_\infty\cos\theta$ and $u_{cy} - U_\infty\sin\theta$, respectively, yielding

$$P_{\phi x} = \frac{\pi}{4}b(b+c)(u_{cx} - U_\infty\cos\theta), \tag{2.12}$$

$$P_{\phi y} = \frac{\pi}{4}c(b+c)(u_{cy} - U_\infty\sin\theta). \tag{2.13}$$

Substituting (2.12) and (2.13) back into (2.10), and assuming the free-stream velocity to be steady, i.e. $\mathrm{d}U_\infty/\mathrm{d}t = 0$, we obtain the following after differentiation and algebraic manipulation:

$$F_x = \frac{\pi}{4}\rho c^2\left\{U_\infty\frac{\mathrm{d}\theta}{\mathrm{d}t}\left(1-\frac{b^2}{c^2}\right)\sin\theta - u_{cy}\frac{\mathrm{d}\theta}{\mathrm{d}t} - \frac{b^2}{c^2}\frac{\mathrm{d}u_{cx}}{\mathrm{d}t}\right\}, \tag{2.14}$$

$$F_y = \frac{\pi}{4}\rho c^2\left\{U_\infty\frac{\mathrm{d}\theta}{\mathrm{d}t}\left(1-\frac{b^2}{c^2}\right)\cos\theta + u_{cx}\frac{b^2}{c^2}\frac{\mathrm{d}\theta}{\mathrm{d}t} - \frac{\mathrm{d}u_{cy}}{\mathrm{d}t}\right\}. \tag{2.15}$$

Note that when $\mathrm{d}\theta/\mathrm{d}t = 0$, these expressions collapse to the original ones given in (2.4) and (2.5), even when $U_\infty \neq 0$. When normalized by $1/2\rho cU_\infty^2$, the force coefficients become

$$C_x = \frac{\pi}{2}\left\{\frac{\mathrm{d}\theta}{\mathrm{d}t^*}\left(1-b^{*2}\right)\sin\theta - u_{cy}^*\frac{\mathrm{d}\theta}{\mathrm{d}t^*} - b^{*2}\frac{\mathrm{d}u_{cx}^*}{\mathrm{d}t^*}\right\}, \tag{2.16}$$

$$C_y = \frac{\pi}{2}\left\{\frac{\mathrm{d}\theta}{\mathrm{d}t^*}\left(1-b^{*2}\right)\cos\theta + u_{cx}^*b^{*2}\frac{\mathrm{d}\theta}{\mathrm{d}t^*} - \frac{\mathrm{d}u_{cy}^*}{\mathrm{d}t^*}\right\}, \tag{2.17}$$

where $t^* = tU_\infty/c$, $b^* = b/c$ and the velocities have been normalized by U_∞.

https://doi.org/10.1017/jfm.2021.741 Published online by Cambridge University Press

Equations (2.16) and (2.17) provide the promised general expressions for the added-mass force on an elliptic airfoil. One colleague has remarked (and I agree) that it is surprising not to find this result long established. It is of wide applicability and seems unlikely to have escaped the interest of the early pioneers of aerodynamics. One might speculate that it had to await the tidy expression of the added-mass force in terms of a surface integral, as in (2.2) and in the monograph of Saffman (1992). Earlier derivations of the added-mass force have treated the changing kinetic energy in the unbounded fluid domain, calculating the work done on the fluid to determine the force, e.g. Brennen (1982) and Lighthill (1986). That approach suffers from the non-convergence of the energy integral when the velocity is non-zero in the far field, and thus the general effects of rotation would be difficult to capture in closed form.

In the following section, it will be shown how (2.16) and (2.17) recover Theodorsen's (1935) non-circulatory lift on thin airfoils as a special case.

3. Generalizing the non-circulatory lift of Theodorsen (1935)

Theodorsen (1935) derived the lift on an oscillating thin airfoil using potential flow theory. He assumed small-amplitude motions consisting of pitching about a fixed point on the chord line, located at x_p relative to the mid-chord ($x_p < 0$ for a pivot point ahead of the mid-chord), and plunging of the pivot point transversely to the free-stream direction. (He also considered a third degree of freedom with which we are not herein concerned: a pitching aileron mounted to the trailing edge.) The vertical velocity of the pivot point is denoted by V_p, normalized as $V_p^* = V_p/U_\infty$.

Theodorsen's non-circulatory component of the lift coefficient, C_L, expressed in the notation of the present work, is

$$C_L = \frac{\pi}{2}\left\{\frac{\mathrm{d}\theta}{\mathrm{d}t^*} - \frac{\mathrm{d}V_p^*}{\mathrm{d}t^*} - x_p^*\frac{\mathrm{d}^2\theta}{\mathrm{d}t^{*2}}\right\}. \tag{3.1}$$

When attempting to generalize for large θ, recent literature has suggested that Theodorsen's expression is rightly applied to the chord-normal rather than stream-normal direction (Polet, Rival & Weymouth 2015; Otomo *et al.* 2021), which is now corroborated. Setting $u_{cy}^* = V_p^*\cos\theta + x_p^*\mathrm{d}\theta/\mathrm{d}t^*$, and $b^* = 0$ in (2.17), we obtain the general expression for chord-normal force coefficient on a thin airfoil:

$$C_y = \frac{\pi}{2}\left\{\cos\theta\frac{\mathrm{d}\theta}{\mathrm{d}t^*} + V_p^*\sin\theta\frac{\mathrm{d}\theta}{\mathrm{d}t^*} - \frac{\mathrm{d}V_p^*}{\mathrm{d}t^*}\cos\theta - x_p^*\frac{\mathrm{d}^2\theta}{\mathrm{d}t^{*2}}\right\}. \tag{3.2}$$

Invoking the small-angle approximations $\sin\theta \approx \theta$ and $\cos\theta \approx 1$, we recover something similar to (3.1):

$$C_y \approx \frac{\pi}{2}\left\{\frac{\mathrm{d}\theta}{\mathrm{d}t^*} + V_p^*\theta\frac{\mathrm{d}\theta}{\mathrm{d}t^*} - \frac{\mathrm{d}V_p^*}{\mathrm{d}t^*} - x_p^*\frac{\mathrm{d}^2\theta}{\mathrm{d}t^{*2}}\right\}. \tag{3.3}$$

The second term above is absent in Theodorsen's formulation, but an order-of-magnitude analysis justifies its neglect. For harmonic motions with a pitch amplitude of θ_0, we have the first term of order $O(\mathrm{d}\theta/\mathrm{d}t^*) \sim O(k\theta_0)$, where k is the reduced frequency. The second term is of order $O(k^2 h_0^*\theta_0^2)$, where h_0^* is the chord-normalized plunge amplitude, such that this term may have a magnitude similar to or greater than that of the first if $O(h_0^*) \gg 1$ or $O(k) \gg 1$. However, the third term is of order $O(k^2 h_0^*)$, which will always be greater than

https://doi.org/10.1017/jfm.2021.741 Published online by Cambridge University Press

h_0^*	θ_0	Φ	x_p^*	f^*
3/8	$\{15^\circ, 35^\circ, 55^\circ, 75^\circ\}$	$\pi/2$	$-1/2$	0.32

Table 1. Parameters of harmonic motion for thin-airfoil ($b^* = 0$) test cases to be compared in figures 2(a) and 2(b): h_0^* is chord-normalized plunge amplitude, θ_0 is pitch amplitude, Φ is the phase difference between the plunge and pitch motions, x_p^* is chord-normalized pivot point location and f^* is normalized frequency.

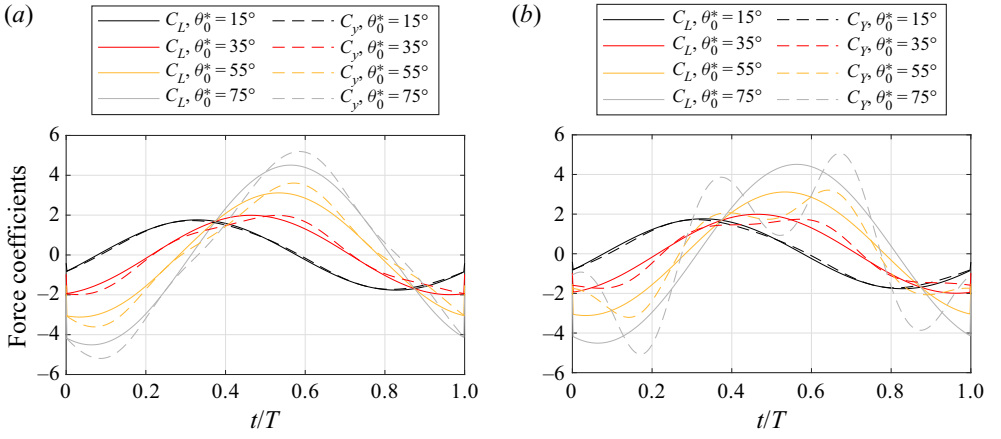

Figure 2. (a) Chord-normal added-mass force (C_y) for thin airfoils from (3.2) and Theodorsen's C_L from (3.1) versus period-normalized time t/T for the pitching and plunging motions characterized in table 1. (b) Stream-normal added-mass force (C_Y) from (3.6), and C_L versus t/T for the same airfoil motions.

that of the second term so long as $\theta_0 \ll 1$. Thus, for any plunge amplitude and frequency, Theodorsen's expression is a good approximation for small pitch angles.

Remarkably, at least for some cases, Theodorsen remains an adequate approximation of the chord-normal added-mass force even at high pitch angles. As an example, we take the motion of a high-efficiency flapping-wing propulsion experiment from Van Buren, Floryan & Smits (2019) and increase the pitch amplitude from 15° to 75° in increments of 20°. The combined pitching and plunging motion is characterized by the following five normalized parameters: chord-normalized plunge amplitude, h_0^*; pitch amplitude, θ_0; pivot location lying on the chord-line, x_p^*; normalized frequency, $f^* = fc/U_\infty$; and the phase difference between the plunging and pitching motions, Φ, defined such that if the plunge position is

$$Y_p^* = h_0^* \sin(2\pi f^* t^*), \tag{3.4}$$

then

$$\theta = \theta_0 \sin(2\pi f^* t^* + \Phi). \tag{3.5}$$

The kinematic parameters for these test cases are given in table 1.

Figure 2(a) shows that the chord-normal force trend over one period of motion, T, is well captured by Theodorsen, although instantaneous deviations are notable; for the extreme case of $\theta_0 = 75^\circ$, the maximum instantaneous difference between C_y and C_L is 23 % of the root-mean-square value of C_y.

https://doi.org/10.1017/jfm.2021.741 Published online by Cambridge University Press

Qualitative and quantitative agreement between Theodorsen and the stream-normal added-mass force,

$$C_Y = C_y \cos\theta - C_x \sin\theta, \tag{3.6}$$

is poorer for these same pitch amplitudes, as shown in figure 2(*b*). This is due to the chord-wise component of the added-mass force, C_x, which is often overlooked but does appear in some general treatments, e.g. Sedov (1965), Limacher *et al.* (2018) and Van Buren *et al.* (2019). With the same substitutions and simplifications as were made to obtain C_y for thin airfoils, (2.16) yields

$$C_x = \frac{\pi}{2}\frac{\mathrm{d}\theta}{\mathrm{d}t^*}\left\{\sin\theta - V_p^*\cos\theta - x_p^*\frac{\mathrm{d}\theta}{\mathrm{d}t^*}\right\}, \tag{3.7}$$

which vanishes as expected for $\mathrm{d}\theta/\mathrm{d}t^* = 0$.

4. Recovering the circular cylinder case

For the limiting case of $b^* = 1$, our general force equations must reduce to the well-known added-mass force on a circular cylinder. Because of its rotational symmetry, the force on a circular cylinder, expressed in the inertial frame, can have no dependence on $\mathrm{d}\theta/\mathrm{d}t^*$; that is, a rotation of the cylinder about its centre has no effect on the surrounding irrotational flow. Setting $b^* = 1$, the first rotation-dependent terms in (2.16) and (2.17) vanish, and we are left with

$$\begin{bmatrix} C_x \\ C_y \end{bmatrix} = -\frac{\pi}{2}\frac{\mathrm{d}\theta}{\mathrm{d}t^*}\begin{bmatrix} u_{cy}^* \\ -u_{cx}^* \end{bmatrix} + \frac{\pi}{2}\frac{\mathrm{d}}{\mathrm{d}t^*}\begin{bmatrix} u_{cx} \\ u_{cy} \end{bmatrix}. \tag{4.1}$$

The remaining dependence on $\mathrm{d}\theta/\mathrm{d}t^*$ is due only to the rotation of the reference frame. Reversing the procedure carried out in (2.6)–(2.10), (4.1) becomes

$$\begin{bmatrix} C_x \\ C_y \end{bmatrix} = -\frac{\pi}{2}\boldsymbol{R}(\theta)\frac{\mathrm{d}}{\mathrm{d}t^*}\left\{\boldsymbol{R}(-\theta)\begin{bmatrix} u_{cx}^* \\ u_{cy}^* \end{bmatrix}\right\}, \tag{4.2}$$

from which, after rotation, we recover the expected force coefficients expressed in the inertial frame:

$$\begin{bmatrix} C_X \\ C_Y \end{bmatrix} = -\frac{\pi}{2}\frac{\mathrm{d}}{\mathrm{d}t^*}\begin{bmatrix} u_{cX}^* \\ u_{cY}^* \end{bmatrix}. \tag{4.3}$$

5. The effect of thickness for pitching and plunging airfoils

The general expressions given in (2.16) and (2.17) allow us to discuss the effect of airfoil thickness on the added-mass force for some canonical harmonic motions within a steady free-stream flow: pure pitching, pure plunging, and combined pitching and plunging.

Pure plunging is merely a subset of rectilinear translation, for which $\mathrm{d}\theta/\mathrm{d}t^* = 0$ and (2.16) and (2.17) reduce to normalized equivalents of the previously known added-mass forces given in (2.4) and (2.5). Thickness has no effect on the chord-normal added-mass force in this case, and gives rise to a chord-wise component that grows as b^{*2}.

For pure pitching about the mid-chord, $x_p^* = 0$ and $u_{cx}^* = u_{cy}^* = 0$, and the force coefficients reduce to the first terms on the right-hand sides of (2.16) and (2.17). This reveals that increasing thickness will reduce both C_x and C_y by the same factor, and the greatest force magnitude for any given $\theta = \theta(t^*)$ will be achieved when $b^* = 0$.

For pure pitching about a point lying on the chord-line at $x_p^* \neq 0$, $u_{cy} \neq 0$ but $u_{cx}* = du_{cx}/dt^* = 0$. Accordingly, we once again find that increasing thickness can only decrease

https://doi.org/10.1017/jfm.2021.741 Published online by Cambridge University Press

Study	b^*	h_0^*	θ_0	Φ	x_p^*	f^*
Kinsey & Dumas (2008)	$\{0, 0.1, 0.2, 0.3\}$	1	75°	$\pi/2$	$-1/6$	0.15
Van Buren *et al.* (2019)	$\{0, 0.1, 0.2, 0.3\}$	3/8	15°	$\pi/2$	$-1/2$	0.32

Table 2. Airfoil thicknesses to be considered, and chosen kinematic parameters for pitching and plunging test cases from recent studies to be compared in figures 3(*a*) and 3(*b*).

the force magnitude in both directions by modifying the first terms on the right-hand sides of (2.16) and (2.17) .

For the general three-degree-of-freedom case, increasing thickness can either increase or decrease the instantaneous forces, but, for any given motion of the chord-line, the difference in force between a thin and a thick airfoil will always be proportional to b^{*2}. That is, if we express the force coefficients for a given motion as a function of b^*, i.e. $C_x = C_x(b^*)$, $C_y = C_y(b^*)$, then the instantaneous thickness effects can be stated as

$$C_x(b^*) - C_x(0) = -\frac{\pi}{2} b^{*2} \left(\frac{\mathrm{d}\theta}{\mathrm{d}t^*} \sin\theta + \frac{\mathrm{d}u_{cx}^*}{\mathrm{d}t^*} \right), \tag{5.1}$$

$$C_y(b^*) - C_y(0) = -\frac{\pi}{2} b^{*2} \frac{\mathrm{d}\theta}{\mathrm{d}t^*} (\cos\theta - u_{cx}^*). \tag{5.2}$$

In the static coordinate system, the thickness effects take the form

$$C_X(b^*) - C_X(0) = -b^{*2} f_X \left(\theta, u_{cx}^*, \frac{\mathrm{d}\theta}{\mathrm{d}t^*}, \frac{\mathrm{d}u_{cx}^*}{\mathrm{d}t^*} \right), \tag{5.3}$$

$$C_Y(b^*) - C_Y(0) = -b^{*2} f_Y \left(\theta, u_{cx}^*, \frac{\mathrm{d}\theta}{\mathrm{d}t^*}, \frac{\mathrm{d}u_{cx}^*}{\mathrm{d}t^*} \right), \tag{5.4}$$

where the functions f_X and f_Y can yield positive or negative values depending on the instantaneous values of the independent kinematic parameters $u_{cx}^* = u_{cx}^*(t^*)$ and $\theta = \theta(t^*)$ and their derivatives. Interestingly, thickness effects are independent of u_{cy}^* in general.

To give an idea of the possible relative magnitude of the thickness effects, two practical example cases of pitching and plunging airfoils are presented: a high-efficiency case from the propulsion study of Van Buren *et al.* (2019), and the best-performing case from the flapping-wing turbine study of Kinsey & Dumas (2008). The kinematic parameters of these harmonic motions, as previously introduced in § 3, are listed in table 2. In the design of flapping-wing propulsors and flapping-wing turbines, the stream-wise and stream-normal forces (C_X and C_Y) are often the most relevant, and these are plotted in figure 3. The effect of thickness can be characterized by the ratios of peak force magnitudes, defined as

$$r_X = \frac{\max(|C_X(b^*)|)}{\max(|C_X(b^* = 0)|)}, \quad r_Y = \frac{\max(|C_Y(b^*)|)}{\max(|C_Y(b^* = 0)|)}. \tag{5.5a,b}$$

These ratios are plotted against b^* in figure 4. For the thickest airfoil considered ($b^* = 0.3$), the most significant effect was a 21 % decrease in peak C_Y for the Kinsey & Dumas (2008) case.

The above results suggest that thickness effects are of secondary importance compared to the effect of airfoil motion on force, and the expressions in (5.1) and (5.2) may serve adequately as approximate corrections for finite-thickness effects for airfoils of

https://doi.org/10.1017/jfm.2021.741 Published online by Cambridge University Press

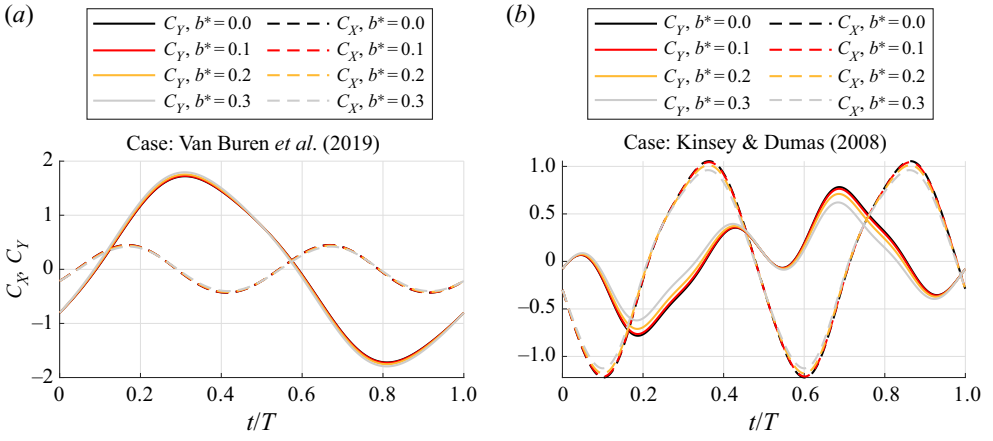

Figure 3. Stream-wise and stream-normal added-mass forces, C_X and C_Y, versus t/T for the test cases listed in table 2.

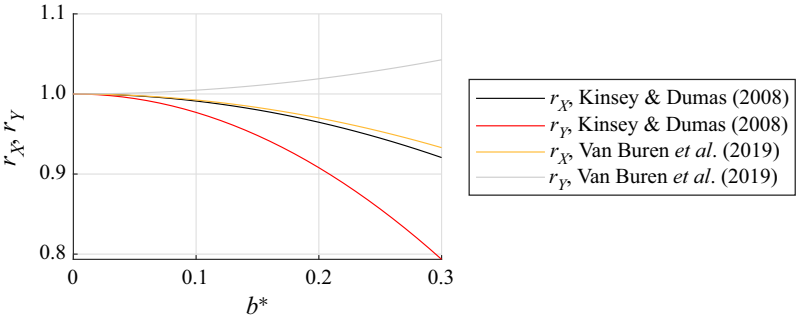

Figure 4. Peak added-mass force magntiude ratios, r_X and r_Y, as defined in (5.5*a*,*b*), versus b^* for the test cases listed in table 2.

other cross-sections. If more exact expressions are desired, the procedure outlined in § 2 can be applied to any rotationally symmetric two-dimensional body; take the known added-mass forces in response to orthogonal components of the body's acceleration, and follow the steps presented in (2.10)–(2.15) to account for body rotation and the presence of a non-zero free-stream flow. To extend this approach to airfoils that do not exhibit rotational symmetry, as is the case with most practical airfoils possessing a sharp trailing edge, definitional differences amongst classical added-mass force analyses must first be addressed, as explained in the Appendix.

6. Conclusion

Exact algebraic expressions for the non-circulatory (added-mass) forces on elliptic airfoils were derived herein for any two-dimensional motion – including one rotational and two linear degrees of freedom – embedded in a steady free stream; see (2.16) and (2.17). These tidy closed-form equations, expressed in terms of geometric and kinematic parameters alone, have wide applicability – covering thin airfoils, circular cylinders and everything in between – but have remained absent from the literature despite the lengthy history of the added-mass concept.

https://doi.org/10.1017/jfm.2021.741 Published online by Cambridge University Press

As airfoil thickness tends to zero, a generalized form of Theodorsen's added-mass force for rigid thin airfoils is recovered in (3.2), applicable to the chord-normal direction; for small pitch angles, this equation collapses to Theodorsen's original expression. The generalized added-mass force for thin airfoils includes a component aligned with the chord – equation (3.7) – which has been established in the literature but is sometimes overlooked. It was shown that, in at least one case, Theodorsen's original expression captures the chord-normal added-mass force trend surprisingly well even at pitch angles up to 75° (although instantaneous deviations are notable), but the chord-wise force becomes a significant contributor to the stream-normal force that cannot be neglected.

Inspection of (2.16) and (2.17) elucidates the effect of airfoil thickness. For purely pitching airfoils with a pivot point lying on the chord-line, increasing thickness always decreases the instantaneous force magnitude in both the chord-wise and chord-normal directions, with the reduction proportional to the square of the chord-normalized thickness, b^{*2}. For combined pitching and plunging, non-zero thickness may either increase or decrease the instantaneous forces relative to a thin airfoil, but the difference remains proportional to b^{*2}. In considering example pitching and plunging test cases from previous flapping-airfoil studies, the most significant observed effect was a decrease of 21 % in the peak stream-normal added-mass force when airfoil thickness was increased from zero to $0.3c$, where c is the chord length.

Funding. The author would like to thank the Natural Sciences and Engineering Research Council of Canada (NSERC) for financial support. This work was also supported under ONR Grant No. N00014-14-1-0533 and N00014-21-1-2210 (Program Manager R. Brizzolera).

Declaration of interests. The author reports no conflict of interest.

Author ORCIDs.
Eric J. Limacher https://orcid.org/0000-0002-1391-6208.

Appendix. Boundary conditions used in defining the classical added-mass force

In Limacher *et al.* (2018), a Helmholtz decomposition was applied to the continuous velocity field of a viscous, incompressible flow. Using vortical impulse theory, it was shown that the rotational component of the velocity field gives rise to a so-called circulatory force, while the irrotational component is associated with the classical added-mass force.

In the decomposition chosen by Limacher *et al.* (2018), the kinematic effect of body rotation was incorporated into the rotational component of the velocity field, so that the irrotational component did not need to satisfy a boundary condition on S that included the surface-normal velocity due to body rotation. This convention stands in contrast to works such as La Mantia & Dabnichki (2012) and Fernandez-Feria (2019), the latter citing the earlier work of Newman (1977) within the marine literature. Fortunately, this definitional difference does not affect the added-mass force expressions derived in the body of the present paper, as is now proven.

The local velocity of any point on the solid body is expressible as $\boldsymbol{u}_c + \boldsymbol{\Omega} \times \boldsymbol{x}$, where $\boldsymbol{\Omega}$ is the body rotation rate and $\boldsymbol{x}$ is the position vector relative to the body centroid. The scalar potential in the body of the paper includes the effect of translation, so let us define a second potential describing the flow induced by rotation only, which can be linearly superimposed onto the first. This second potential, ϕ_Ω, must satisfy the boundary conditions $\nabla\phi_\Omega = 0$ at infinity and $\boldsymbol{n} \cdot \nabla\phi_\Omega = \boldsymbol{n} \cdot (\boldsymbol{\Omega} \times \boldsymbol{x})$ on S.

https://doi.org/10.1017/jfm.2021.741 Published online by Cambridge University Press

Fortunately, we need not solve for this potential flow field to see that its effect on the added-mass force on elliptic airfoils is nil. The potential ϕ_Ω will contribute

$$\oint_S \boldsymbol{n}\phi_\Omega \, \mathrm{d}S \tag{A1}$$

to the potential impulse in (2.2), whose time derivative will yield a force, but this integral vanishes by symmetry: for any point on S, the value of ϕ_Ω will be equal to its value on the point directly opposite (i.e. the point mirrored across both the major and minor axes of the ellipse), while the normal vectors at these two points will be of opposite signs. Even more generally, for bodies exhibiting n-fold rotational symmetry ($n \geq 2$), every point on S belongs to a set of n points for which this cancellation holds, causing the integral in (A1) to vanish.

Going forward, as one seeks to extend the approach presented herein to other airfoils that do not exhibit rotational symmetry, the appropriate definition of the classical added-mass force, and the corresponding boundary conditions, must be clarified in the context of total force decompositions.

References

Brennen, C.E. 1982 A review of added mass and fluid inertial forces. *Tech. Rep.* N62583-81-MR-554. Naval Civil Engineering Laboratory.

Chang, C.-C. 1992 Potential flow and forces for incompressible viscous flow. *Proc. R. Soc. Lond. Ser.* A*: Math. Phys. Sci.* **437** (1901), 517–525.

Fackrell, S. 2011 Study of the added mass of cylinders and spheres. PhD thesis, University of Windsor.

Fernandez-Feria, R. 2019 On the added-mass force and moment and the vortex projection method. Application to thin airfoils. *Fluid Dyn. Res.* **51** (3), 035509.

von Kármán, T. & Sears, W.R. 1938 Airfoil theory for non-uniform motion. *J. Aeronaut. Sci.* **5** (10), 379–390.

Kinsey, T. & Dumas, G. 2008 Parametric study of an oscillating airfoil in a power-extraction regime. *AIAA J.* **46** (6), 1318–1330.

La Mantia, M. & Dabnichki, P. 2012 Added mass effect on flapping foil. *Engng Anal. Bound. Elem.* **36** (4), 579–590.

Lighthill, J. 1986 Fundamentals concerning wave loading on offshore structures. *J. Fluid Mech.* **173**, 667–681.

Limacher, E.J. 2019 Added mass and vortical impulse: theory and experiment. PhD thesis, University of Calgary.

Limacher, E., Morton, C. & Wood, D. 2018 Generalized derivation of the added-mass and circulatory forces for viscous flows. *Phys. Rev. Fluids* **03**, 014701.

Milne-Thomson, L.M. 1968 *Theoretical hydrodynamics*, 5th ed. MacMillan Education Ltd.

Newman, J.N. 1977 *Marine hydrodynamics*. MIT Press.

Ōtomo, S., Henne, S., Mulleners, K., Ramesh, K. & Viola, I.M. 2021 Unsteady lift on a high-amplitude pitching aerofoil. *Exp. Fluids* **62** (1), 6.

Polet, D.T., Rival, D.E. & Weymouth, G.D. 2015 Unsteady dynamics of rapid perching manoeuvres. *J. Fluid Mech.* **767**, 323–341.

Quartapelle, L. & Napolitano, M. 1983 Force and moment in incompressible flows. *AIAA J.* **21** (6), 911–913.

Saffman, P.G. 1992 *Vortex dynamics*. Cambridge University Press.

Sedov, L.I. 1965 *Two-dimensional problems in hydrodynamics and aerodynamics*. Interscience Publishers (John Wiley and Sons Inc.).

Theodorsen, T. 1935 General theory of aerodynamic instability and the mechanism of flutter. *Tech. Rep.* 496. National Advisory Committee for Aeronautics.

Van Buren, T., Floryan, D. & Smits, A.J. 2019 Scaling and performance of simultaneously heaving and pitching foils. *AIAA J.* **57** (9), 3666–3677. arXiv:1801.07625.

Williamson, C.H.K. & Govardhan, R. 2004 Vortex-induced vibrations. *Annu. Rev. Fluid Mech.* **36**, 413–455.

Wu, J.C. 1981 Theory for aerodynamic force and moment in viscous flows. *AIAA J.* **19** (4), 432–441.

Wu, J.-Z., Ma, H.-Y. & Zhou, M.-D. 2015 *Vortical flows*. Springer.

https://doi.org/10.1017/jfm.2021.741 Published online by Cambridge University Press